

## Supporting Information

### **Force-responsive      ordered      carbonaceous      frameworks synthesized from Ni-porphyrin**

Koki Chida,<sup>a</sup> Takeharu Yoshii,<sup>a</sup> Kazuma Takahashi,<sup>a</sup> Masanori Yamamoto,<sup>a</sup> Kazuya Kanamaru,<sup>a</sup> Mao Ohwada,<sup>a</sup> Varisara Deerattrakul,<sup>b</sup> Jun Maruyama,<sup>c</sup> Kazuhide Kamiya,<sup>d, e</sup> Yuichiro Hayasaka,<sup>f</sup> Masataka Inoue,<sup>g</sup> Fumito Tani,<sup>g</sup> and Hiroto Nishihara<sup>\*a, h</sup>

<sup>a</sup> *Institute of Multidisciplinary Research for Advanced Materials, Tohoku University, 2-1-1 Katahira, Aoba, Sendai, Miyagi, 980-8577, Japan.*

<sup>b</sup> *National Nanotechnology Centre (NANOTEC), National Science and Technology Development Agency (NSTDA), Pathum Thani, 12120, Thailand.*

<sup>c</sup> *Research Division of Environmental Technology, Osaka Research Institute of Industrial Science and Technology, 1-6-50 Morinomiya, Joto-ku, Osaka, 536-8553, Japan.*

<sup>d</sup> *Graduate School of Engineering Science, Osaka University, 1-3 Machikaneyama, Toyonaka, Osaka, 560-8531, Japan.*

<sup>e</sup> *Research Centre for Solar Energy Chemistry, Osaka University, 1-3 Machikaneyama, Toyonaka, Osaka, 560-8531, Japan.*

<sup>f</sup> *The Electron Microscopy Centre, Tohoku University, 2-1-1 Katahira, Aoba, Sendai, Miyagi, 980-8577, Japan.*

<sup>g</sup> *Institute for Materials Chemistry and Engineering, Kyushu University, 744 Motooka, Nishi-ku, Fukuoka, 819-0395, Japan.*

<sup>h</sup> *Advanced Institute for Materials Research (WPI-AIMR), Tohoku University, 2-1-1 Katahira, Aoba, Sendai, Miyagi, 980-8577, Japan.*

## Experimental Section

### Materials

Reagents and solvents of the best grade available were purchased from commercial suppliers and were used without further purification unless otherwise noted.

### Synthesis of [5, 10, 15, 20-tetrakis(3,5-diethynylphenyl)porphinato] nickel(II) (Ni-P\_8e (5))

The freebase porphyrin, which possesses eight ethynyl groups, was synthesized according to the literatures,<sup>1, 2</sup> and the overall synthetic procedure was shown in Scheme S1. Ethynyl groups were introduced by Sonogashira coupling.<sup>3</sup> 3,5-Dibromobenzaldehyde (**1**, 5.00 g, 19.0 mmol) was dissolved in a mixture of 1,4-dioxane (super dehydrated, 46.4 ml), Pd(PhCN)<sub>2</sub>Cl<sub>2</sub> (0.458 g, 1.19 mmol), CuI (0.148 g, 0.78 mmol), PPh<sub>3</sub> (0.548 g, 2.09 mmol), *i*Pr<sub>2</sub>NH (6.38 mL, 45.5 mmol) and TMS acetylene (6.40 mL, 46.3 mmol). Sonication was applied to the mixture. The mixture solution was stirred at room temperature for 1 day under Ar. Next, CH<sub>3</sub>COOC<sub>2</sub>H<sub>5</sub> (150 mL) was added to the mixture, and the precipitation was removed by filtration. After removing solvent from the filtrate, the residue was purified by column chromatography with an eluent (hexane/dichloromethane = 1/1) on silica gel, and then 3,5-bis((trimethylsilyl)ethynyl)benzaldehyde (TMSBA, **2**, 4.49 g, 79%) was obtained as the intermediate after drying under vacuum.

<sup>1</sup>H NMR (400 MHz, CDCl<sub>3</sub>,)  $\delta$  9.94 (s, 1H), 7.88 (d, *J* = 1.6 Hz, 2H), 7.79 (t, *J* = 1.6 Hz, 1H), 0.25 (s, 18H).

The aldehyde **2** (1.78 g, 5.95 mmol) was dissolved in propionic acid (27 mL), and then a mixture of pyrrole (0.413 mL, 5.95 mmol) and propionic acid (2.68 mL) was added to the solution including **2**. The reaction mixture was heated up to 413 K under Ar and refluxed under air at 413 K for 3 h. CH<sub>3</sub>OH was added to the mixture after cooling to room temperature, then the precipitate was filtered and washed with CH<sub>3</sub>OH. Finally, H-P\_8e\_TMS (**3**, 787 mg, 19.1%) was obtained as a strong purple powder after vacuum drying at 313 K.

<sup>1</sup>H NMR (400 MHz, CDCl<sub>3</sub>,)  $\delta$  8.86 (s, 8H), 8.27 (s, 8H), 8.07 (s, 4H), 0.30 (s, 72H), -2.91 (s, 2H).

For the Ni insertion process, **3** (69.2 mg, 50.0  $\mu$ mol) and Ni(OCOCH<sub>3</sub>)<sub>2</sub>·4H<sub>2</sub>O (1.4 g, 5.6 mmol) were refluxed in a mixture solution of toluene (super dehydrated, 11.5 mL) and *N,N*-dimethylformamide (super dehydrated, 11.5 mL) under Ar at 413 K for 2 days. Then, the mixture was dissolved in toluene and washed with D.I water. The separated organic phase was dried over Na<sub>2</sub>SO<sub>4</sub>, filtered, and evaporated under vacuum. The residue was purified by column chromatography with an eluent (hexane/dichloromethane = 9/1) on silica gel, and Ni-P\_8e\_TMS (**4**, 61.9 mg, 86%) was obtained after under vacuum drying at 313 K. For the deprotection process, the as-synthesized Ni-P\_8e\_TMS (**4**, 61.9 mg) was dissolved in dichloromethane (68.8 mL) and methanol (68.8 mL). Then, K<sub>2</sub>CO<sub>3</sub> (3.4 g, 25 mmol) was added to this solution and stirred for 2.5 h. After evaporation, the residue was dissolved in CHCl<sub>3</sub> and washed with D.I water, and then recrystallized from dichloromethane and methanol. Finally, Ni-P\_8e (**5**) was obtained as a purple (34.1 mg, 79%) solid after vacuum drying at 313 K.

$^1\text{H}$  NMR (400 MHz,  $\text{CDCl}_3$ )  $\delta$  8.72 (s, 8H), 8.12 (d, 8H,  $J = 1.5$  Hz), 7.98 (t, 4H,  $J = 1.5$  Hz), 3.17 (s, 8H);  $^{13}\text{C}$  NMR (125 MHz,  $\text{CDCl}_3$ )  $\delta$  142.91, 141.37, 137.23, 135.53, 132.52, 121.61, 117.43, 82.58, 78.62; MALDI-TOF-MS  $m/z$  calcd. for  $\text{C}_{60}\text{H}_{28}\text{N}_4\text{Ni}$  862.1662, found 862.196  $[\text{M}]^+$ .

#### Synthesis of [5,10-dimesityl-10,20-di(3-ethynylphenyl)porphinato] nickel (II) (**7**)

The overall synthetic procedure was shown in scheme S2a. The freebase porphyrin, 5,10-dimesityl-10,20-bis(3-trimethylsilylethynylphenyl)porphine (**6**), which possesses two ethynyl groups, was synthesized according to the literature.<sup>4</sup> Overall synthetic scheme was shown in scheme 2. To a solution of **6** (301 mg, 337  $\mu\text{mol}$ ) and 2,6-lutidine (790  $\mu\text{L}$ , 6.80 mmol) in DMF (22 mL) was added  $\text{Ni}(\text{OCOCH}_3)_2 \cdot 4\text{H}_2\text{O}$  (837 mg, 3.36 mmol).<sup>5</sup> The mixture was stirred at 413 K for 2 h under  $\text{N}_2$  in the dark and then cooled to room temperature. To the mixture was added a tetrabutylammonium fluoride solution (1.0 mol  $\text{L}^{-1}$  in THF, 1.35 mL, 1.35 mmol) and then stirred at room temperature for 30 min. The mixture was passed through celite with  $\text{CH}_2\text{Cl}_2$  (100 mL). The filtrate was washed with brine (100 mL) and the aqueous layer was extracted with  $\text{CH}_2\text{Cl}_2$  (50 mL  $\times$  2). The combined organic layer was dried over  $\text{Na}_2\text{SO}_4$ , evaporated and vacuum drying. The crude product was purified by column chromatography on silica gel with an eluent (hexane/ $\text{CH}_2\text{Cl}_2 = 5/1$ ) to give the desired compound (**7**, 214 mg, 79%) as red solids. Crystalline sample for carbonization was prepared as follows. A solution of **7** (214 mg) in  $\text{CH}_2\text{Cl}_2$  (150 mL) was sonicated and MeOH (50 mL) was added. The solution was slowly evaporated at 303 K under vacuum to 50 mL to give red precipitates. The precipitates were filtered and washed with small amount of MeOH followed by drying under vacuum to afford crystalline **7** (167 mg) for carbonization.

$^1\text{H}$  NMR (400 MHz,  $\text{CDCl}_3$ )  $\delta$  8.66 (d,  $J = 5.2$  Hz, 4H), 8.60 (d,  $J = 5.2$  Hz, 4H), 8.17 (s, 2H), 8.04 (d,  $J = 8.0$  Hz, 2H), 7.84 (d,  $J = 8.0$  Hz, 2H), 7.64 (t,  $J = 8.0$  Hz, 2H), 7.21 (s, 4H), 3.14 (s, 2H), 2.58 (s, 6H), 1.80 (s, 12H);  $^{13}\text{C}$  NMR (150 MHz,  $\text{CDCl}_3$ )  $\delta$  142.86, 142.77, 141.53, 139.14, 137.91, 137.30, 137.03, 134.11, 132.41, 131.65, 131.51, 127.93, 127.02, 120.96, 117.87, 117.44, 83.79, 77.62, 21.56, 21.50; HR-FAB-MS  $m/z$  calcd. for  $\text{C}_{54}\text{H}_{40}\text{N}_4\text{Ni}$  802.2606, found 802.2599  $[\text{M}]^+$ ; IR (KBr)  $\nu$  3296, 3128, 1601, 1441, 1377, 1350, 1311, 1209, 1171, 1070, 1003, 922, 901, 858, 835, 798, 756, 729, 715  $\text{cm}^{-1}$ .

#### Synthesis of [5,10-dimesityl-10,20-bis(3,5-diethynylphenyl)porphinato] nickel (II) (**10**)

The overall synthetic procedure was shown in scheme S2b. The freebase porphyrin, 5,10-dimesityl-10,20-bis(3,5-bis(trimethylsilylethynyl)phenyl)porphine (**9**), which possesses four ethynyl groups, was synthesized according to the method of the literature.<sup>4</sup> To a solution of **2** (1.28 g, 4.29 mmol) and *meso*-mesityldipyromethane<sup>6</sup> (**8**, 1.13 g, 4.27 mmol) in  $\text{CHCl}_3$  (563 mL) was added  $\text{BF}_3 \cdot \text{Et}_2\text{O}$  (235  $\mu\text{L}$ , 1.87 mmol). The mixture was stirred at room temperature for 1 h under the  $\text{N}_2$  in the dark. 2,3-Dichloro-5,6-dicyano-*p*-benzoquinone (DDQ, 970 mg, 4.27 mmol) was added to the reaction mixture and stirred at room temperature for 1 h. The mixture was passed through a column of silica gel ( $\text{CHCl}_3$ ) and evaporated under vacuum. The crude product was purified by column chromatography on silica gel

with an eluent (*n*-hexane/CH<sub>2</sub>Cl<sub>2</sub> = 5/1) to give the desired compound (**9**, 1.09 g, 47%) as purple solids.

<sup>1</sup>H NMR (400 MHz, CDCl<sub>3</sub>) δ 8.73 (d, *J* = 4.8 Hz, 4H), 8.70 (d, *J* = 4.8 Hz, 4H), 8.23 (d, *J* = 1.6 Hz, 4H), 8.01 (t, *J* = 1.6 Hz, 2H), 7.29 (s, 4H), 2.64 (s, 6H), 1.83 (s, 12H), 0.25 (s, 36H), -2.72 (s br., 2H); <sup>13</sup>C NMR (150 MHz, CDCl<sub>3</sub>) δ 142.50, 139.49, 138.29, 138.01, 137.01, 136.07, 127.96, 122.05, 118.91, 117.33, 104.20, 95.52, 21.77, 21.62, 0.04 (four aromatic signals were overlapped); HR-FAB-MS *m/z* calcd. for C<sub>70</sub>H<sub>74</sub>N<sub>4</sub>Si<sub>4</sub> 1082.4991, found 1082.4987 [M]<sup>+</sup>; IR (KBr) ν 3309, 2964, 2906, 2154, 1814, 1614, 1585, 1471, 1412, 1375, 1350, 1250, 1221, 1203, 1167, 1072, 1053, 985, 953, 922, 854, 802, 762, 735 cm<sup>-1</sup>.

To a solution of **9** (150 mg, 138 μmol) and 2,6-lutidine (330 μL, 2.84 mmol) in DMF (9.3 mL) was added Ni(OCOCH<sub>3</sub>)<sub>2</sub>·4H<sub>2</sub>O (347 mg, 1.39 mmol). The mixture was stirred at 413 K for 2 h under N<sub>2</sub> in the dark and then cooled to room temperature. To the reaction mixture was added a tetrabutylammonium fluoride solution (1.0 mol L<sup>-1</sup> in THF, 1.15 mL, 1.15 mmol) and then stirred at room temperature for 30 min. The mixture was passed through celite with CH<sub>2</sub>Cl<sub>2</sub> (100 mL). The filtrate was washed with brine (100 mL) and the aqueous layer was extracted with CH<sub>2</sub>Cl<sub>2</sub> (50 mL × 2). The combined organic layer was dried over Na<sub>2</sub>SO<sub>4</sub>, evaporated and dried under vacuum. The crude product was purified by column chromatography on silica gel with an eluent (hexane/CH<sub>2</sub>Cl<sub>2</sub> = 7/1) to give the desired product (**10**, 101 mg, 86%) as red solids. Crystalline sample for carbonization was prepared as follows. A solution of **10** (101 mg) in CH<sub>2</sub>Cl<sub>2</sub> (75 mL) was sonicated and MeOH (25 mL) was added. The solution was slowly evaporated at 303 K to 25 mL to give red precipitates. The precipitates were filtered and washed with small amount of MeOH followed by drying under vacuum to afford crystalline **10** (66.1 mg) for carbonization.; <sup>1</sup>H NMR (400 MHz, CDCl<sub>3</sub>) δ 8.64 (d, *J* = 4.8 Hz, 4H), 8.61 (d, *J* = 4.8 Hz, 4H), 8.14 (d, *J* = 1.6 Hz, 4H), 7.96 (t, *J* = 1.6 Hz, 2H), 7.22 (s, 4H), 3.15 (s, 4H), 2.58 (s, 6H), 1.80 (s, 12H); <sup>13</sup>C NMR (150 MHz, CDCl<sub>3</sub>) δ 143.04, 142.61, 141.85, 139.11, 138.00, 137.16, 137.09, 135.12, 132.23, 131.72, 131.72, 127.95, 121.36, 118.14, 116.35, 82.73, 78.38, 21.56, 21.48; HR-FAB-MS *m/z* calcd. for C<sub>58</sub>H<sub>40</sub>N<sub>4</sub>Ni 850.2606, found 850.2609 [M]<sup>+</sup>; IR (KBr) ν 3469, 3300, 2929, 2864, 1587, 1460, 1352, 1074, 1003, 937, 891, 858, 835, 802, 762, 717 cm<sup>-1</sup>.

Heat treatment of the samples was performed at a heating rate of 10 K min<sup>-1</sup> under N<sub>2</sub> at a specified temperature (553, 873 or 973 K) in a tubular furnace. The sample name after the heat treatment is expressed as follows: Ni-P\_8e\_X(Y) or N\_X(Y) for N is the number of molecule (**7** or **10**), X is the treated temperature (K), and Y is the holding time (h).

### Characterization

<sup>1</sup>H NMR spectra were recorded on a Bruker Avance III 400 spectrometer and a JEOL ECS 400 spectrometer. <sup>13</sup>C NMR spectra were recorded on a Bruker AVANCE III 500 spectrometer and a Bruker AVANCE III 600 spectrometer. Chemical shifts of NMR spectra are reported as δ values in ppm relative to tetramethylsilane. To confirm that the target molecules were certainly obtained, matrix assisted laser

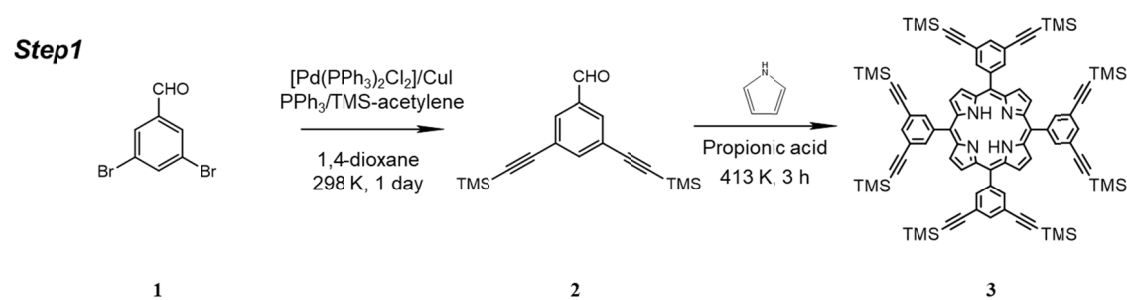
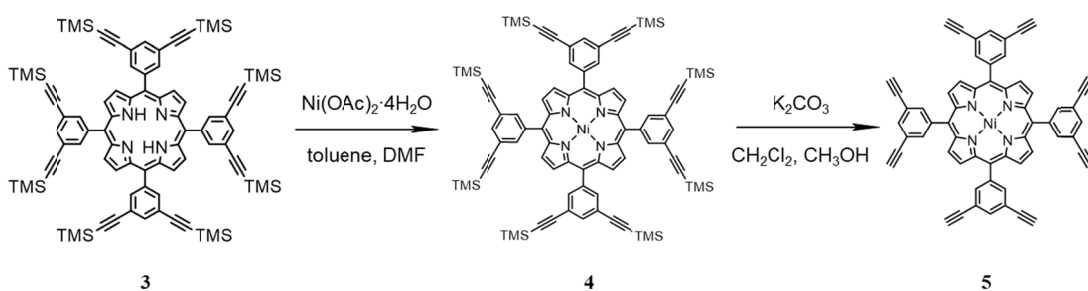
desorption/ionization-time of flight-mass spectroscopy (MALDI-TOF-MS) was conducted on a Bruker Autoflex Speed. High-resolution fast atom bombardment mass spectra (HR-FAB-MS) were recorded on a JEOL JMS-700 spectrometer with 3-nitrobenzyl alcohol (NBA) as a matrix. Infrared (IR) spectra were recorded on a JEOL JIR-WINSPEC50 spectrometer.  $^{13}\text{C}$  cross polymerization-magic angle spinning (CP-MAS) NMR spectra was obtained on a JEOL JNM-ECA800 (800 MHz) spectrometer. Raman spectra were measured on a JASCO Corp NRS-3300FL.

Thermal analysis was carried out using a Thermogravimeter-differential scanning calorimeter (TG-DSC; STA 449 Jupiter, Netzsch) from 333 K to 973 K with a heating rate of  $10\text{ K min}^{-1}$  under a He flow ( $150\text{ mL min}^{-1}$ ). The emission gas from the TG-DSC was analysed with a quadrupole mass spectrometer (MS; JMS-G1500GC, JEOL). For crystalline structure analysis of Ni-P<sub>8e</sub>, a high quality PXRD pattern was obtained on a Rigaku SmartLab diffractometer (Cu-K $\alpha$  radiation, 45 kV, 200 mA,  $1.54059\text{ \AA}$ ). The powder diffraction data were collected between  $2\text{--}60^\circ$  ( $2\theta$ ) with  $0.01^\circ$ . The crystal structure refinement was clarified using the direct space method with the parallel templating algorithm<sup>7</sup> followed by the Rietveld refinement<sup>8</sup>. Crystal structure was analysed using integrated X-ray powder diffraction software (PDXL Version 2.3.1.0, Rigaku). The structure refinement was carried out with a restraint function available in PDXL. Other PXRD patterns were measured using a Rigaku MiniFlex600 (Cu-K $\alpha$  radiation, 40 kV, 15 mA,  $1.5418\text{ \AA}$ ). X-ray photoelectron spectroscopy (XPS) analysis was performed using a JEOL JPS-9200 (Al-K $\alpha$  radiation, spot size = 3 mm). For analysis, binding energy of a peak corresponding to  $sp^2$  carbon was calibrated to  $284.5\text{ eV}$ .<sup>9</sup> Identifications of each chemical species such as C=O, C–N, C–C ( $sp^3$ ), and C–C ( $sp^2$ ) was determined according to literature.<sup>10,11</sup> Transmission electron microscopy (TEM) images were obtained using a JEOL JEM-2010/JEM-2200FS operated at 200 kV. Scanning electron microscopy (SEM) images were obtained on a FE-SEM using a Hitachi-S4800. High angle annular dark field scanning transmission electron microscopy (HAADF-STEM) and the energy-dispersive X-ray spectrometry (EDS)-mapping of Ni-P<sub>8e</sub>\_873(0) were conducted using a Titan<sup>12</sup> G2 60-300 Double Cs-Corrector (FEI company) equipped with an energy-dispersive X-ray spectrometer (Super-X) at an acceleration voltage of 60 kV. Ni K-edge X-ray absorption fine structure (XAFS) spectra were recorded by a transmission mode at the BL14B2 or BL01B1 beamline in SPring-8, JASRI, Harima, Japan, using Si (111) monochromator. Fourier transform was applied to the  $k^3$ -weighted normalized extended X-ray absorption fine structure (EXAFS) data over the range of  $3.0 < k (\text{\AA}^{-1}) < 12$  to obtain radial structure functions using Athena and Artemis.<sup>13</sup>  $\text{N}_2$  adsorption-desorption isotherms were obtained using a MicrotracBEL Corp. BELSORP-max system at 77 K. The Brunauer-Emmett-Teller (BET) surface area was calculated using the multipoint BET method from the adsorption data in the range of  $p/p_0 = 0.01\text{--}0.05$ . The total pore volume was estimated at  $p/p_0 = 0.96$ . The pore-size distributions were calculated with the non-local density functional theory (NLDFT) using a slit-pore model.<sup>14</sup>

#### ***In situ* measurement of liquid-vapour adsorption/desorption behaviour with mechanical pressing**

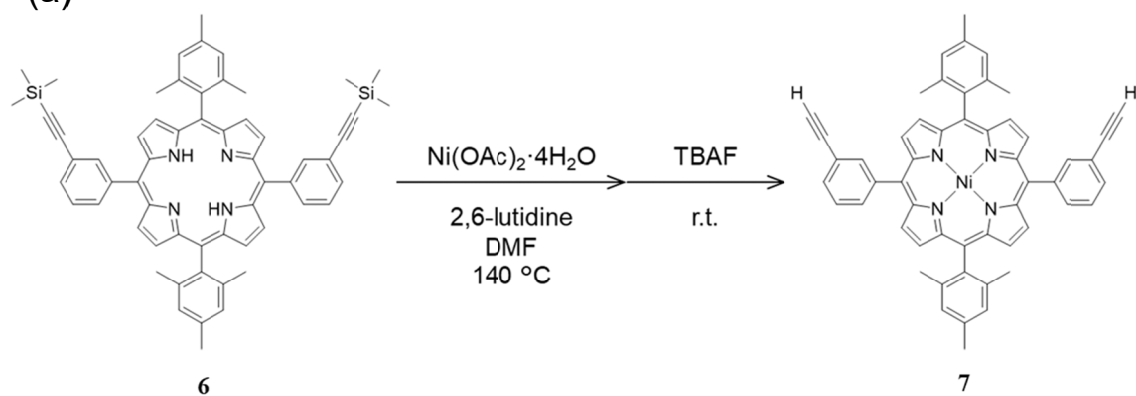
*In situ* vapour adsorption measurement was performed based on the previously-developed system.<sup>15,16</sup> Ni-P<sub>8e\_873(0)</sub> was mixed with PTFE binder (7 wt%) to prepare sample sheets. Several sheets were sandwiched by thin stainless-steel plates to get a sufficient adsorption amount, and then the sample was mounted in a closed chamber which is equipped with a bellows-sealed linear feedthrough (Figure S20). The sheets were degassed at 298 K under vacuum in the chamber connected to an adsorption measurement apparatus (MicrotracBEL Corp., BELSORP-max system). By using the specially designed closed chamber connected to the adsorption measurement apparatus, it is possible to apply a mechanical force to the sample sheets with measuring adsorption/desorption behaviours. Prior to the *in situ* measurement, the sample stack was pressed with 213 MPa to stabilize the elastic deformation.

Two types of *in situ* measurements were performed. The First measurement is liquid-adsorption isotherms of Ni-P<sub>8e\_873(0)</sub> at 298 K with and without the application of mechanical force. The second measurement is the monitoring the vapour pressure of the chamber upon force-driven phase transition of methanol or ethanol on Ni-P<sub>8e\_873(0)</sub> at 298 K. Prior to the second measurement, the liquid-adsorption equilibrium was established on Ni-P<sub>8e\_873(0)</sub> at  $P/P_0 = 0.916$  without application of mechanical force. With continuously monitoring the vapour-phase pressure of the chamber, a mechanical force (213 MPa) was applied to the sample stack for 15 min to compress the nanopores, followed by removal of the force for 10 min to recover the nanopores. The pressing/releasing cycle was repeated three times. When the sample stack is compressed by the linear feedthrough, the dead volume of the chamber is slightly decreased by the movement of the linear feedthrough. To examine the effect of the dead-volume change associated by the movement of the linear feedthrough, we have performed a blank test. The change of vapour pressure was measured when the linear feedthrough was moved by the same degree as that of the *in situ* measurement. The decrease of the dead volume is 0.11 cm<sup>3</sup>, only 0.2% of the total dead volume (56 cm<sup>3</sup>), corresponding to the increase of  $P/P_0$  by 0.015 as shown in Figure S22. Thus, the intense increase of  $P/P_0$  observed in Figure 4b is apparently derived from the force-driven phase transition occurring on Ni-P<sub>8e\_873(0)</sub>.

**Step1****Step2**

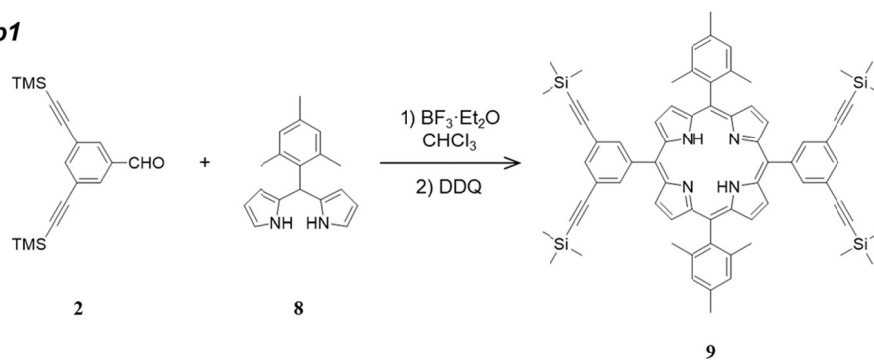
**Scheme S1** Synthetic procedure of Ni-P\_8e (**5**).

(a)

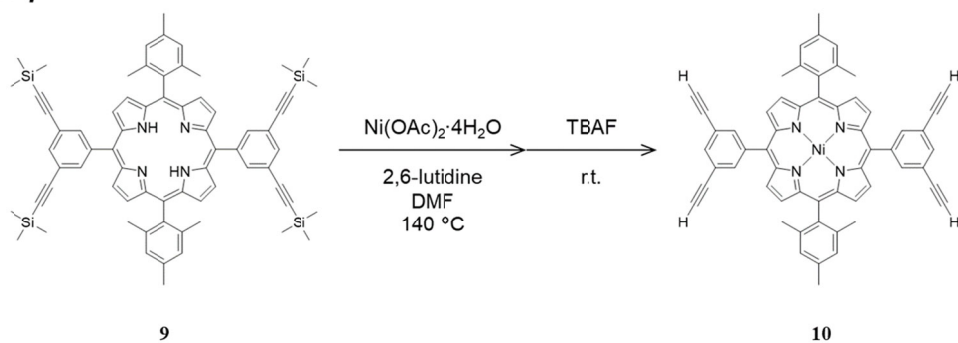


(b)

**Step1**

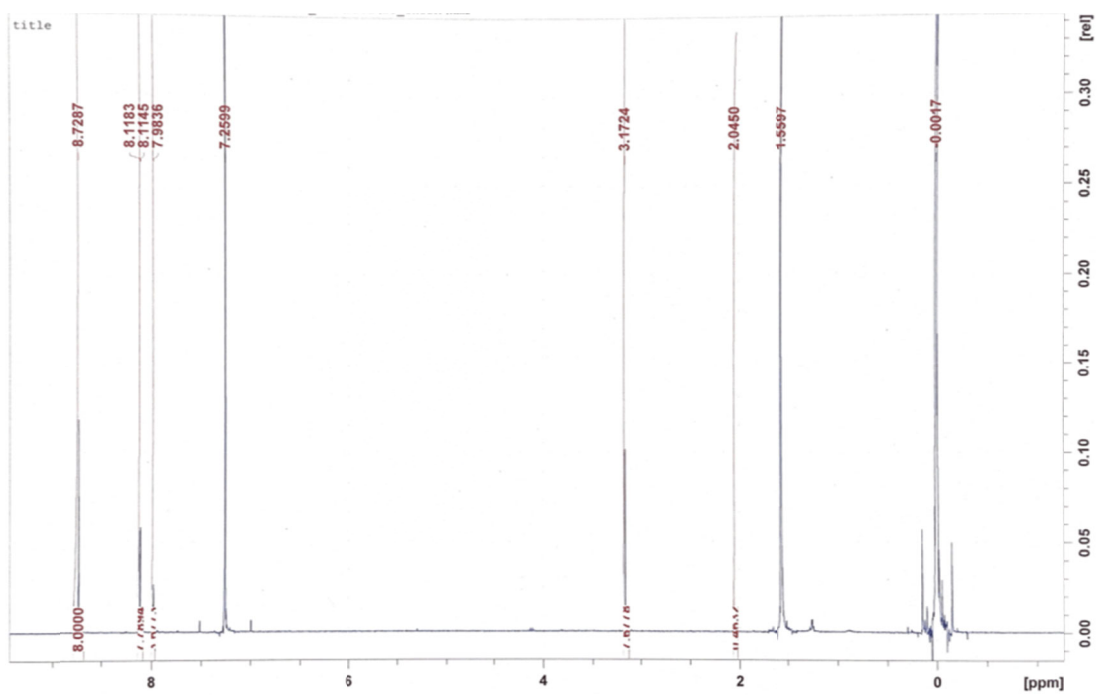


**Step2**

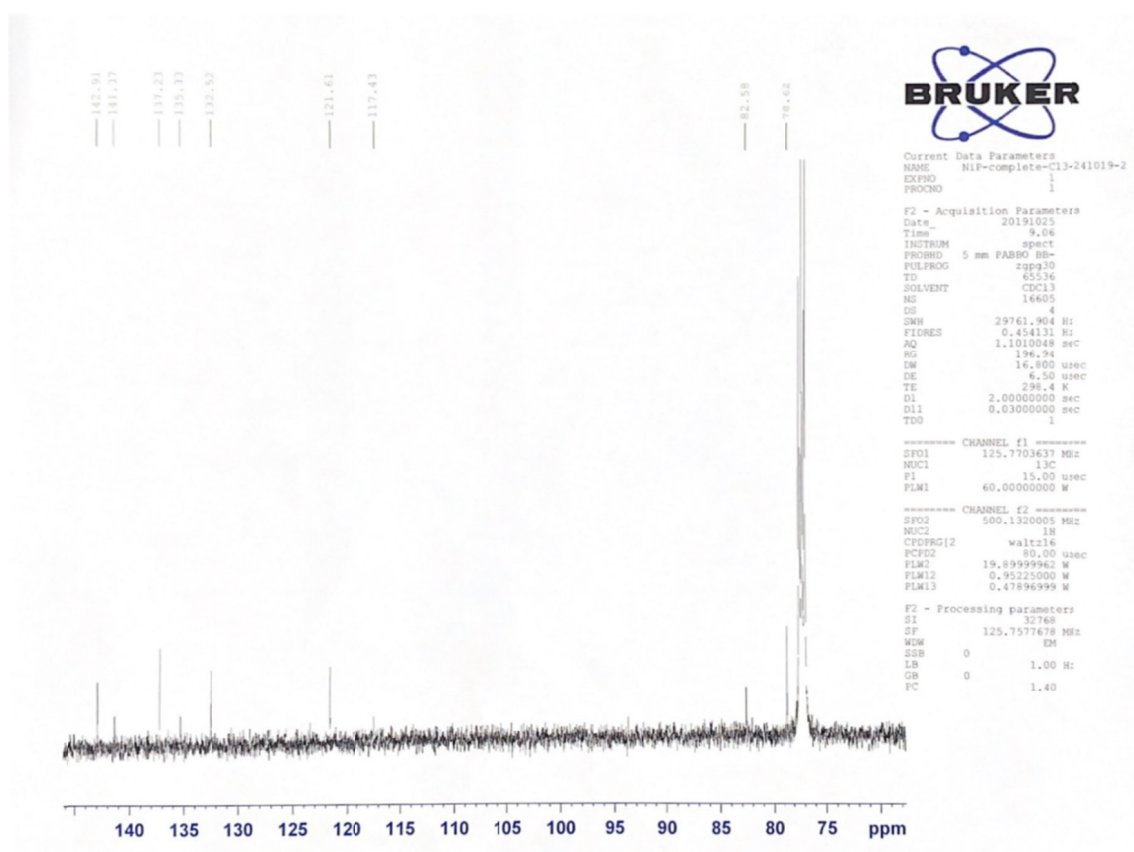


**Scheme S2** Synthetic procedure of (a) **7** and (b) **10**.

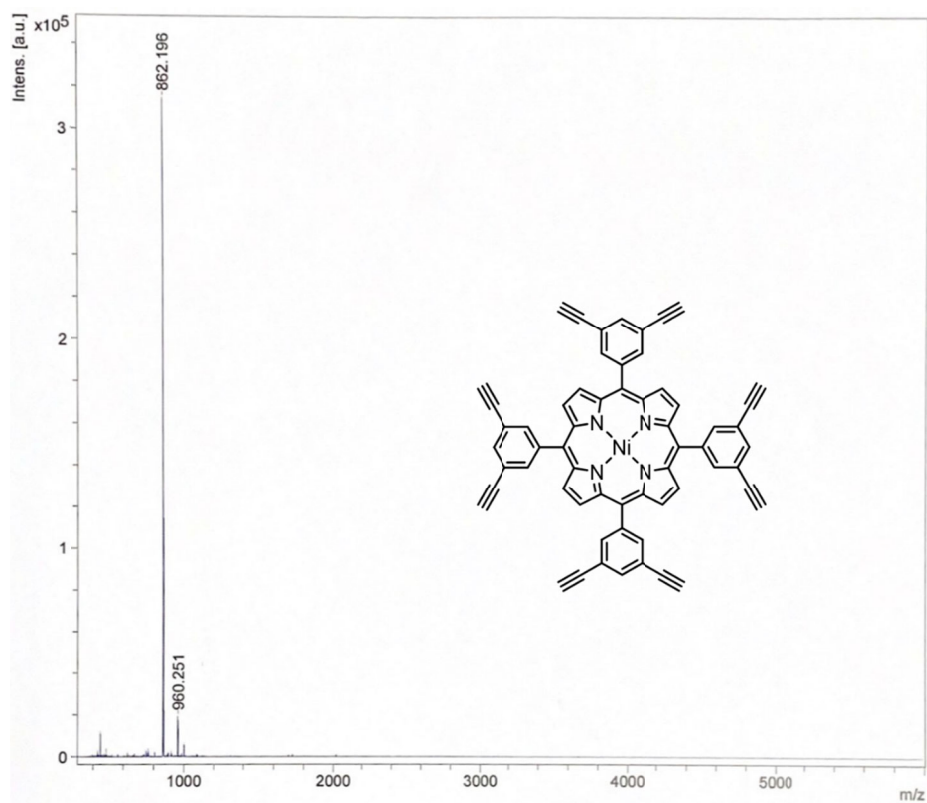




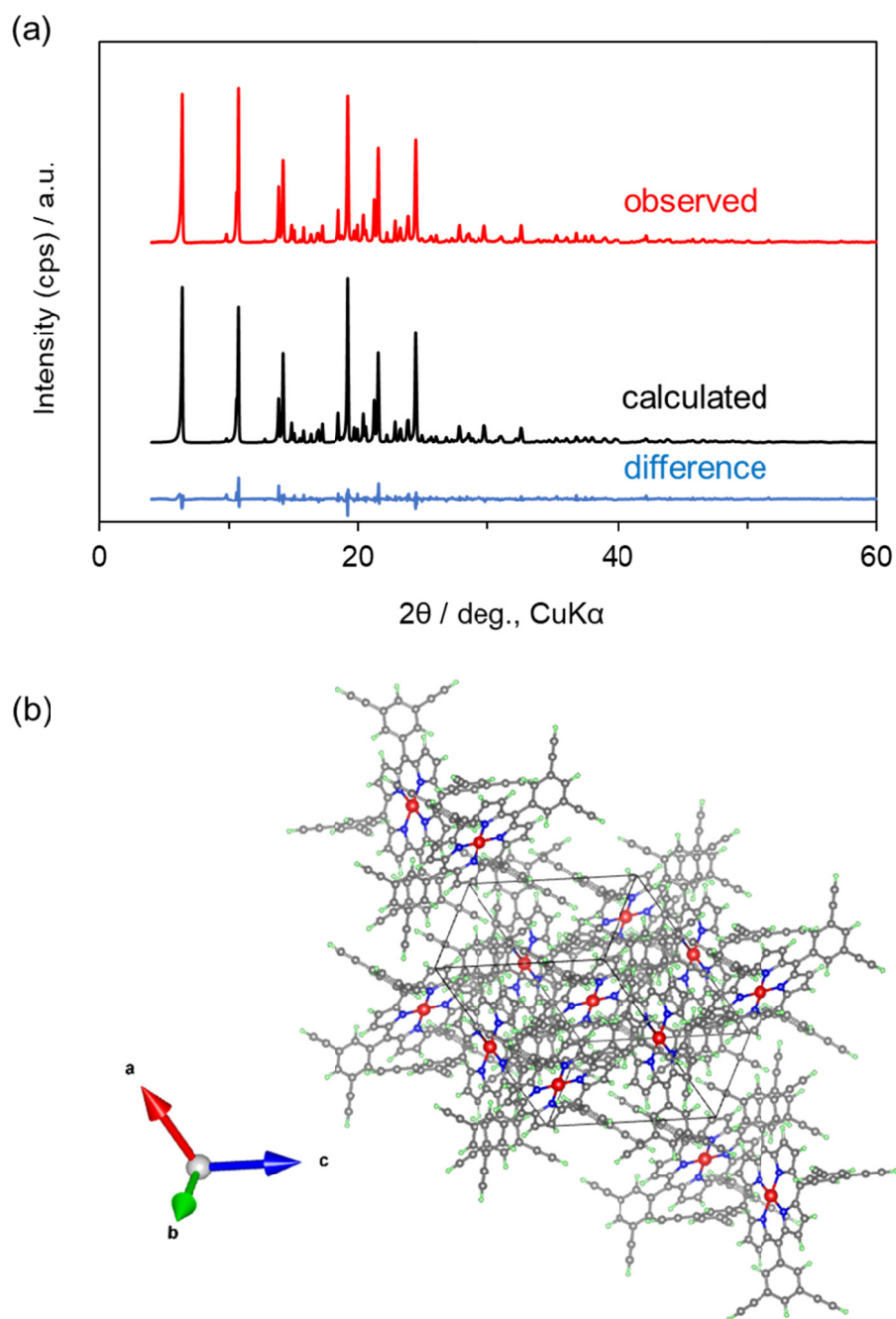
**Figure S1**  $^1\text{H}$  NMR (400 MHz) spectrum of Ni-P<sub>8</sub>e in  $\text{CDCl}_3$ .



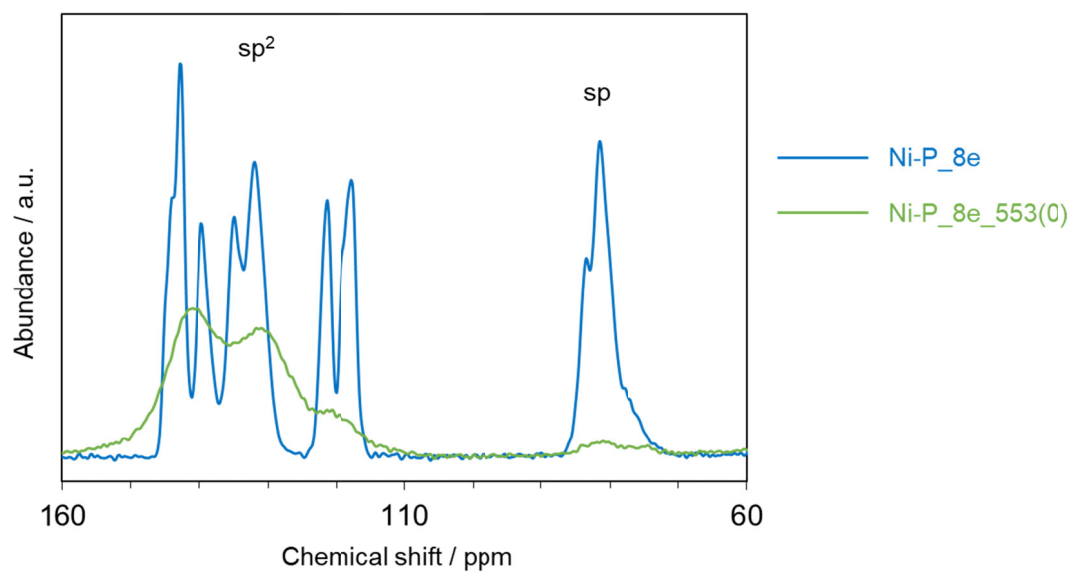
**Figure S2**  $^{13}\text{C}$  NMR (125 MHz) spectrum of Ni-P<sub>8</sub>e in CDCl<sub>3</sub>.



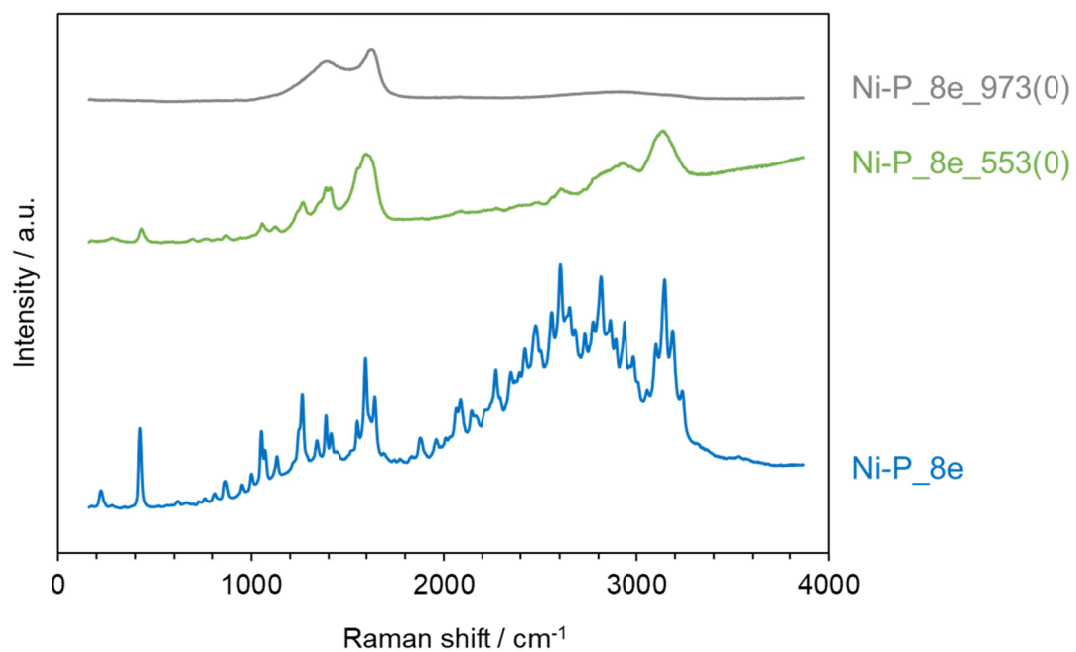
**Figure S3** MALDI-TOF-MS result of Ni-P<sub>8e</sub>.



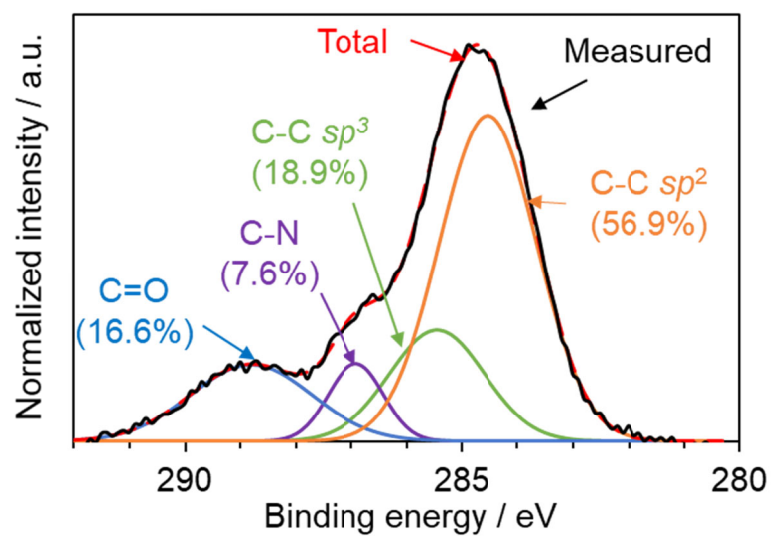
**Figure S4** (a) PXRd pattern and the profile fitting result and (b) crystalline structure of Ni-P\_8e. space group:  $P 2_1/c$ , unit cell volume:  $2106.9 \text{ \AA}^3$ ,  $a = 15.0815 \text{ \AA}$ ,  $b = 11.8280 \text{ \AA}$ ,  $c = 12.8360 \text{ \AA}$ ,  $\beta = 113.055^\circ$ ,  $d_{\text{calc}}: 1.36 \text{ g/cm}^3$ . Crystallographic data (CIF file) have been deposited with the Cambridge Crystallographic Data Centre as supplementary publications (CCDC 2063651).



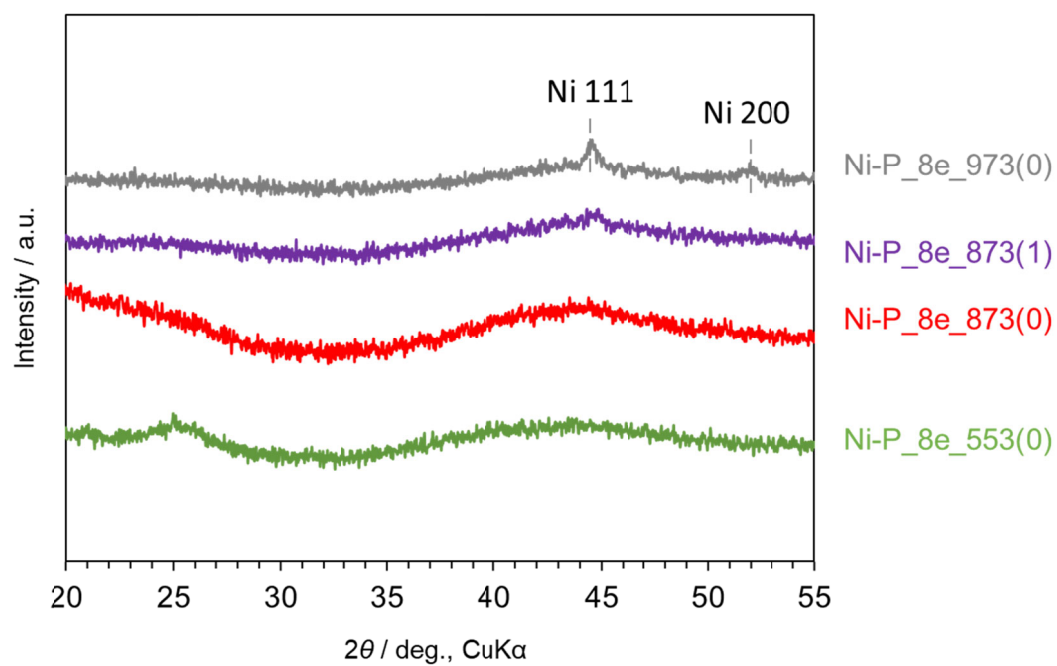
**Figure S5**  $^{13}\text{C}$  NMR spectra of Ni-P<sub>8e</sub> and its heat-treated derivative at 553 K (Ni-P<sub>8e</sub><sub>553(0)</sub>).



**Figure S6** Raman spectra of Ni-P<sub>8e</sub> and its heat-treated derivatives at 553 K (Ni-P<sub>8e</sub>\_553(0)) and 973 K (Ni-P<sub>8e</sub>\_973(0)).

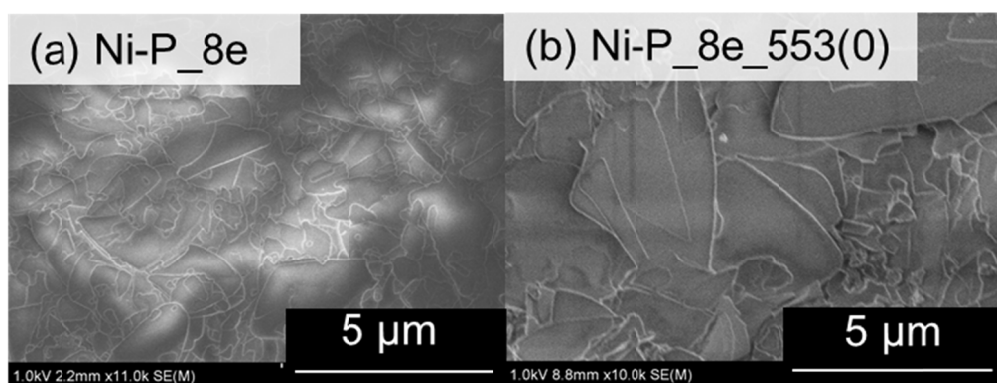


**Figure S7** XPS C1s spectrum of OCF prepared by heat-treatment of Ni-P<sub>8e</sub> at 873 K (Ni-P<sub>8e</sub>\_873(0)).

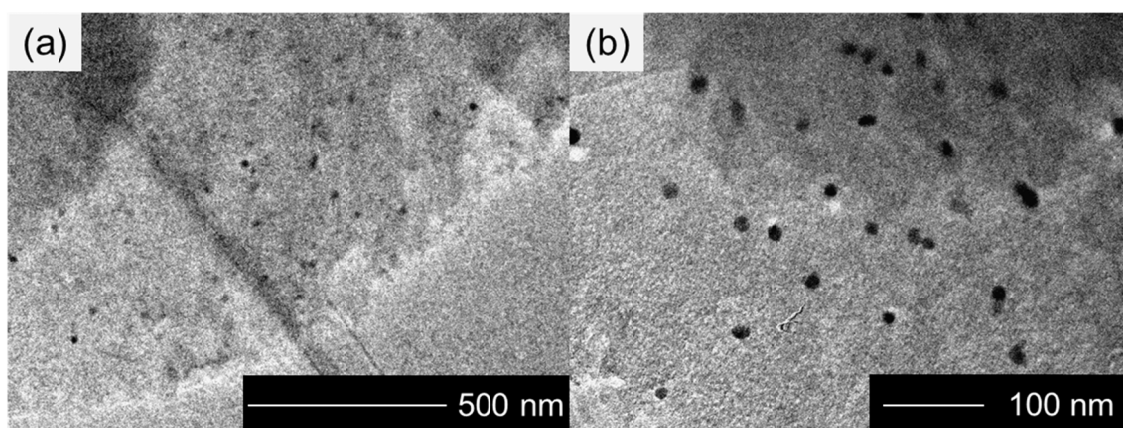


**Figure S8** PXRD patterns ( $2\theta = 20\text{-}55^\circ$ ) of heat-treated samples derived from Ni-P<sub>8e</sub>.

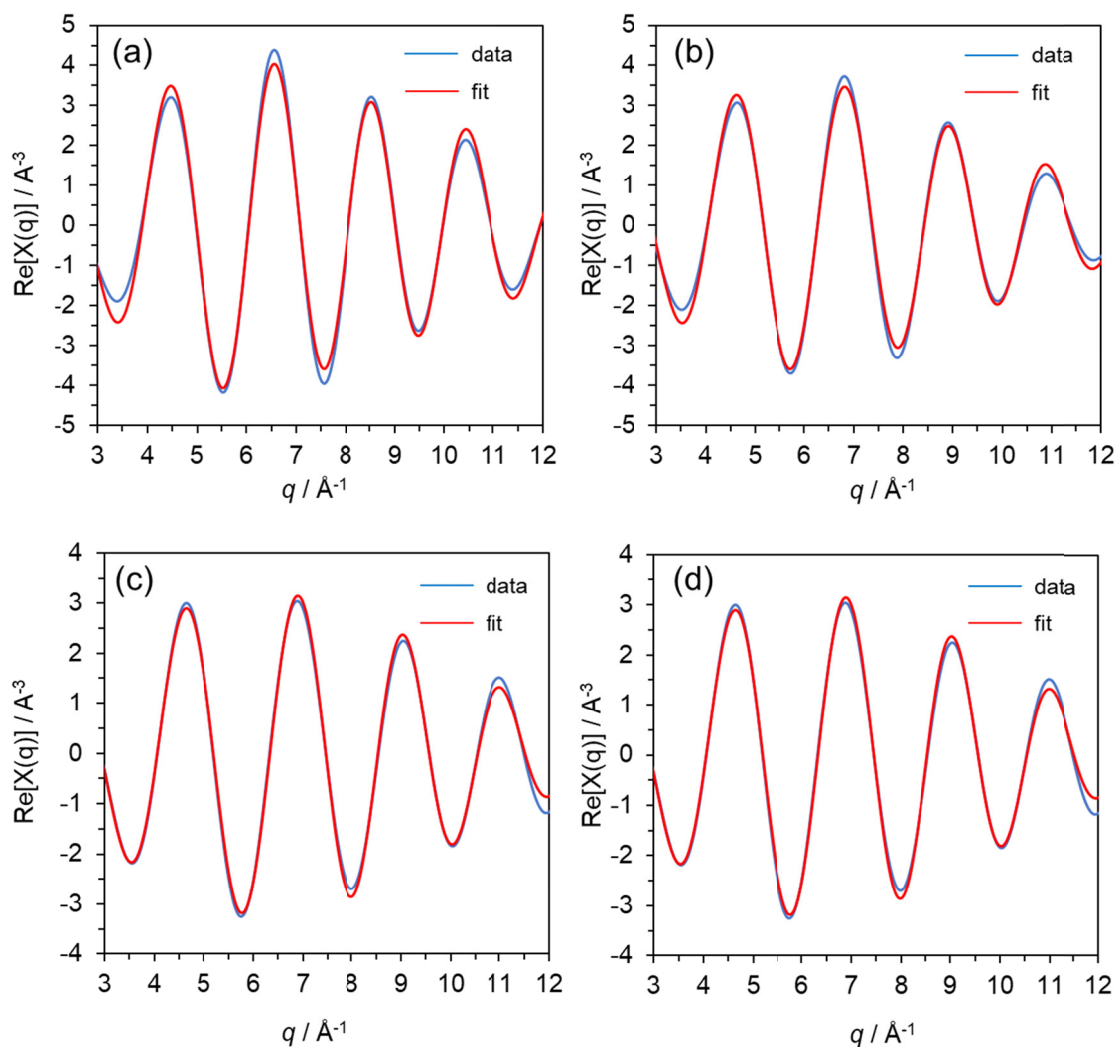




**Figure S9** SEM images of (a) Ni-P<sub>8e</sub> and (b) Ni-P<sub>8e\_553(0)</sub>.

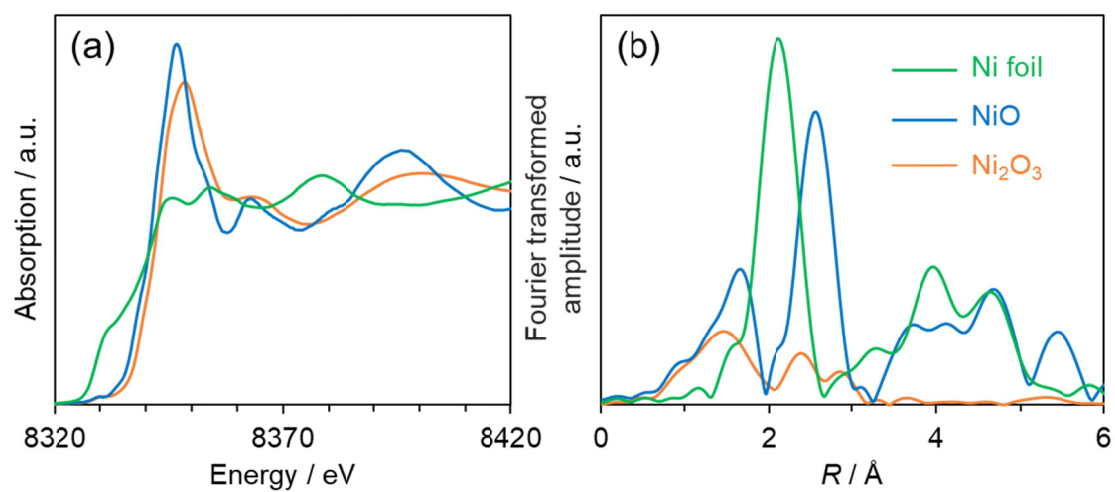


**Figure S10** (a, b) TEM images of Ni-P\_973(0) at different magnifications.



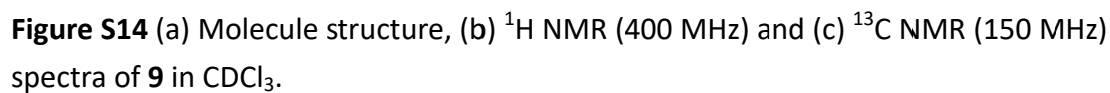
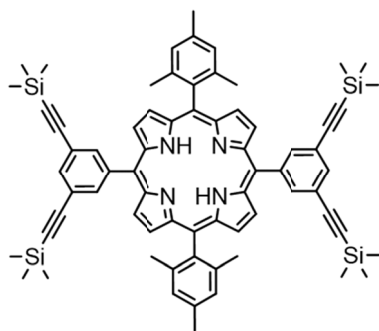
**Figure S11** Ni K-edge extended XAFS oscillation function fitted to Ni-N of (a) Ni-P\_8e, (b) Ni-P\_8e\_873(0), (c) Ni-P\_8e\_873(1) and (d) Ni-P\_8e\_973(0).

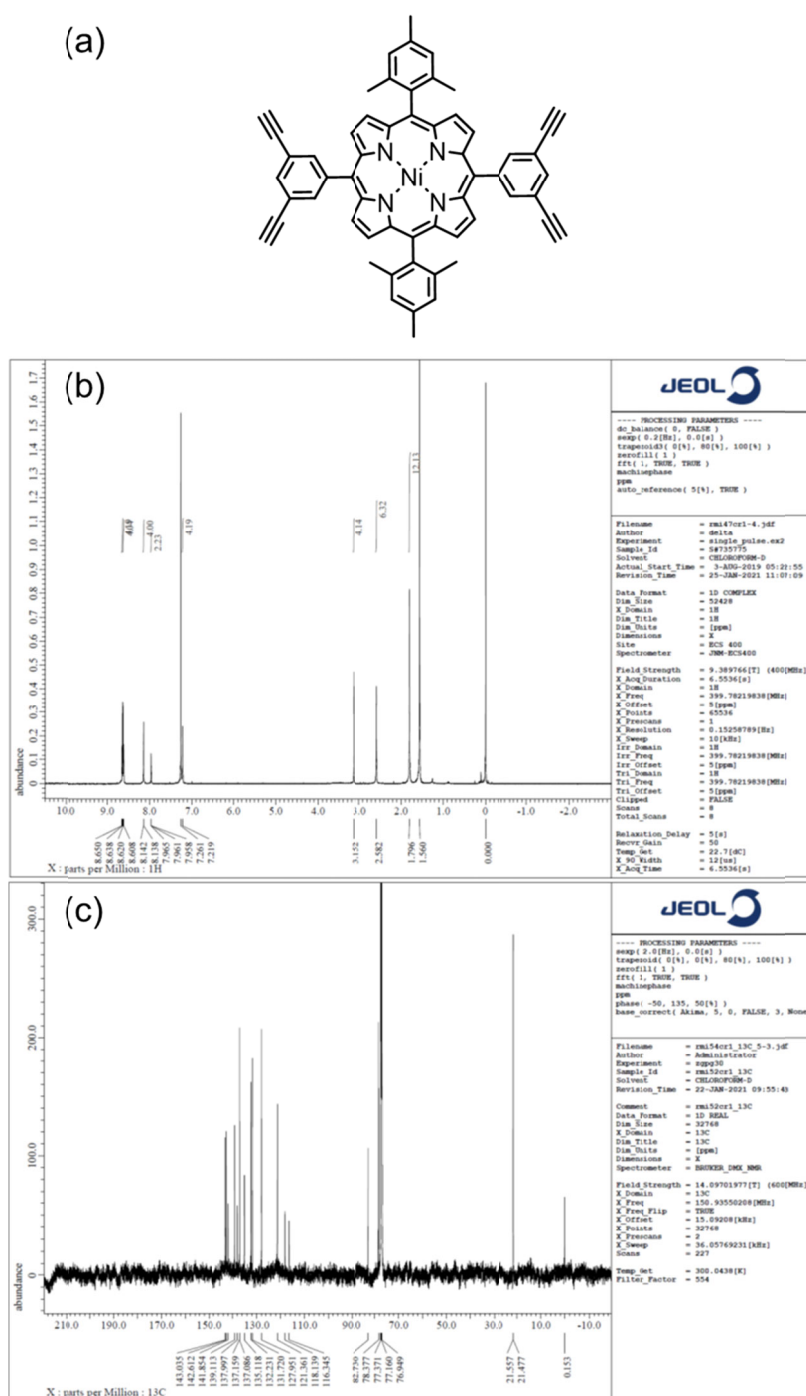
The oscillation functions of EXAFS fitted to  $q$  space are in accordance with data results, indicating the fitting results are reasonable.



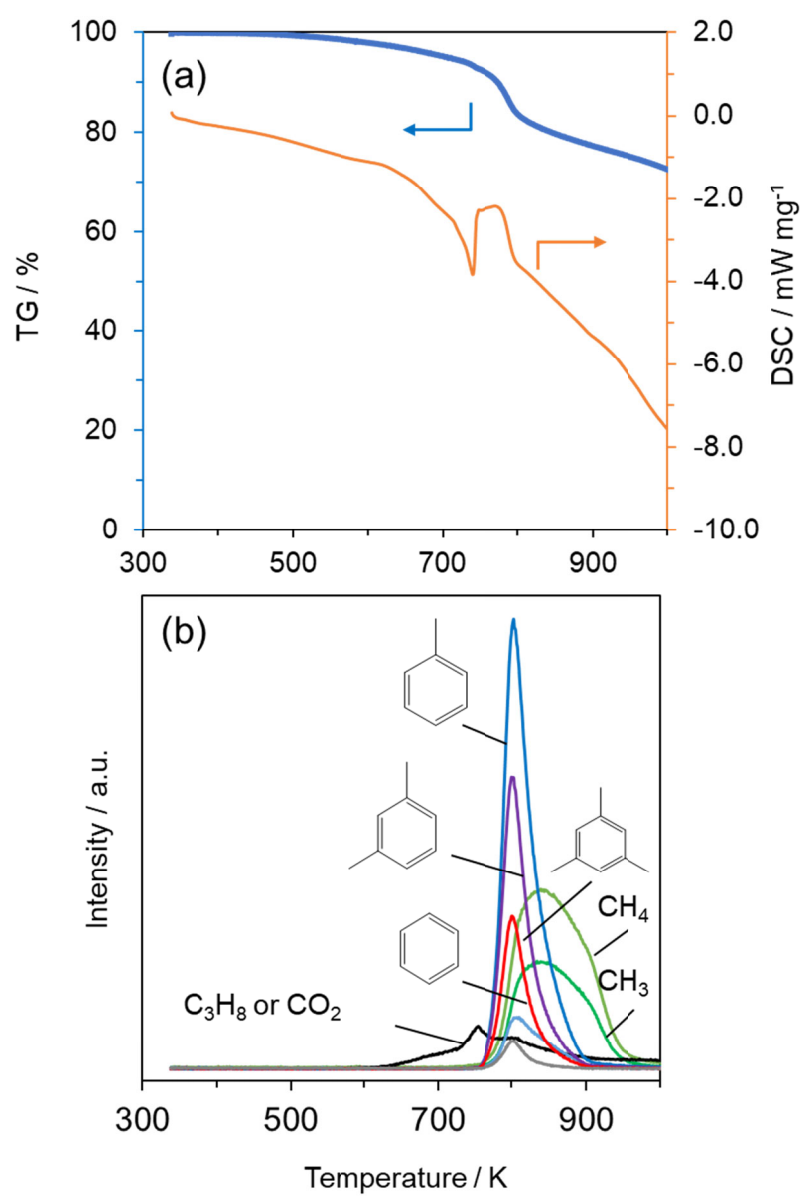
**Figure S12** (a) Ni-K edge XANES spectra and (b) RSFs of Ni-foil, NiO and Ni<sub>2</sub>O<sub>3</sub>.





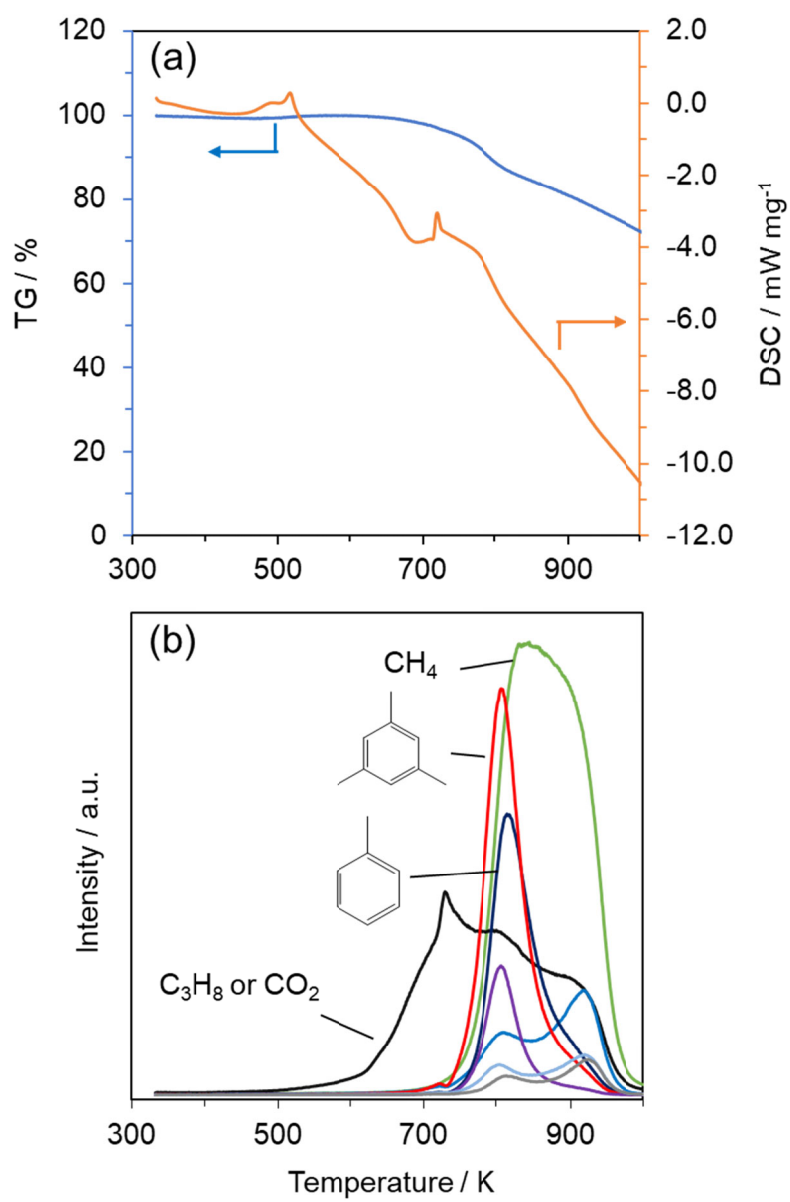


**Figure S15** (a) Molecule structure, (b)  $^1\text{H}$  NMR (400 MHz) and (c)  $^{13}\text{C}$  NMR (150 MHz) spectra of **10** in  $\text{CDCl}_3$ .

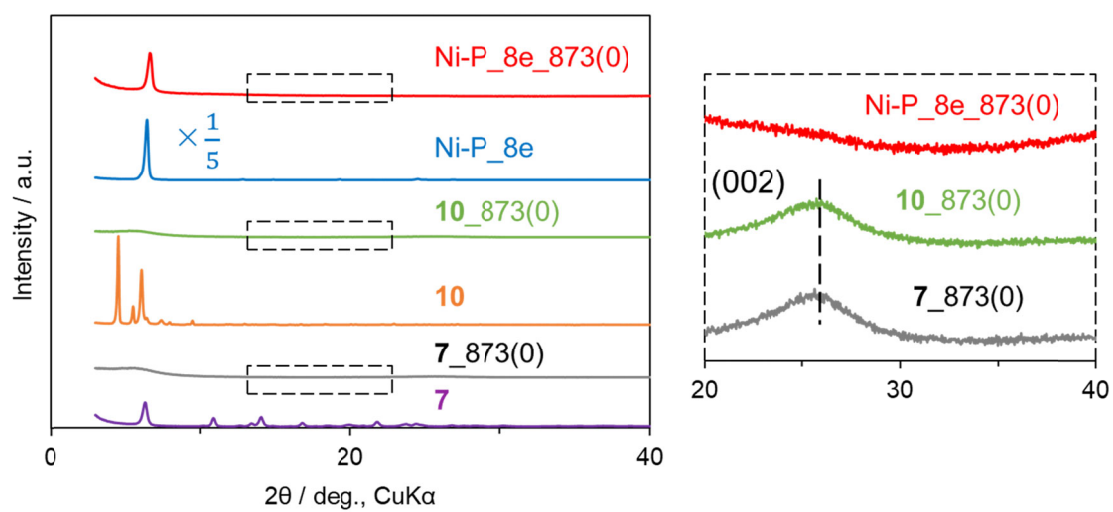


**Figure S16** (a) TG-DSC and (b) MS results of **7**.

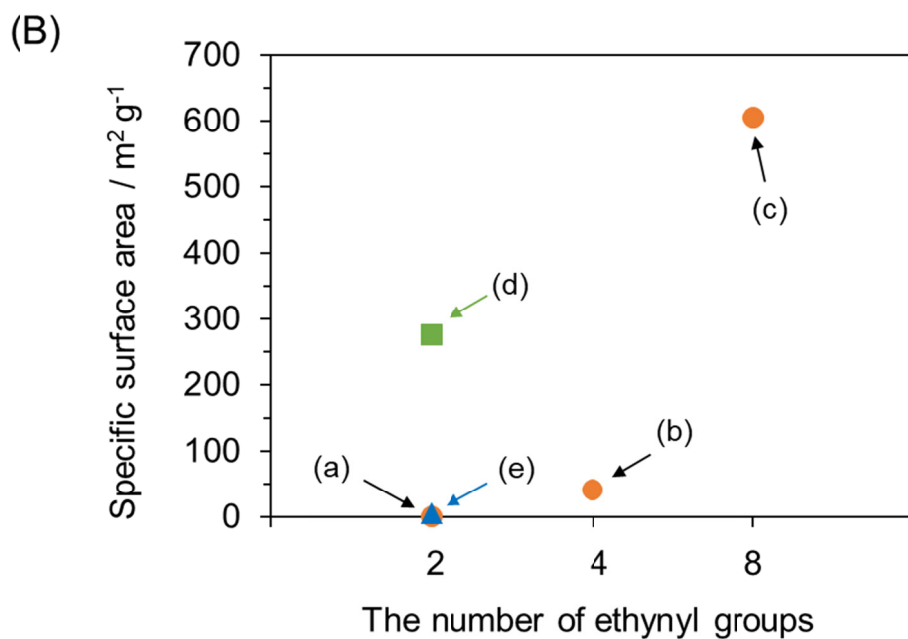
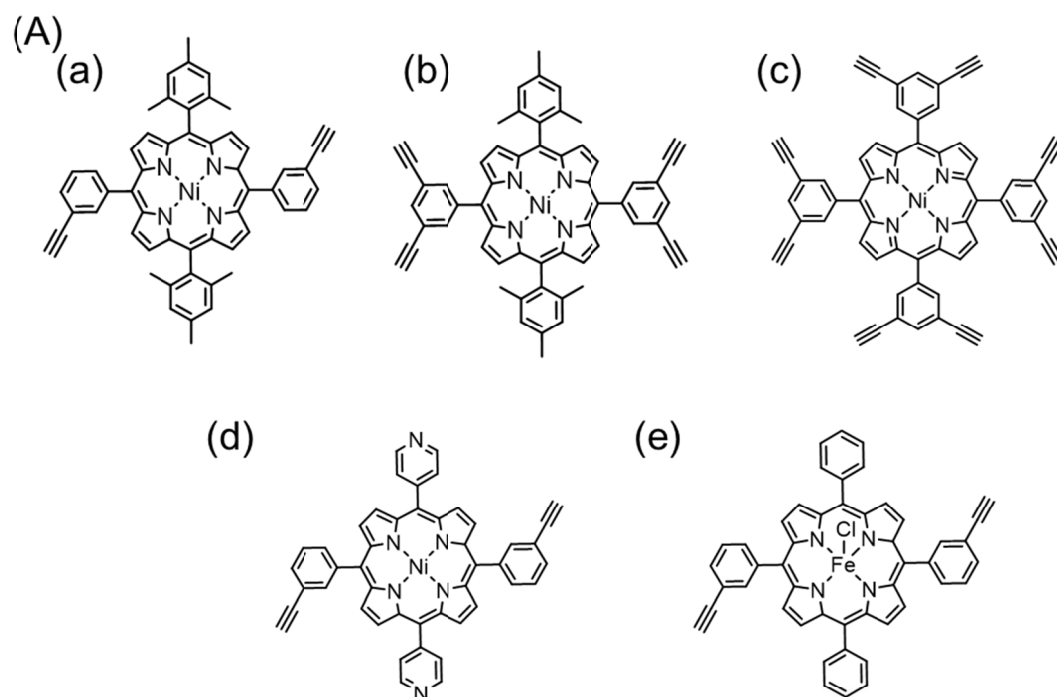




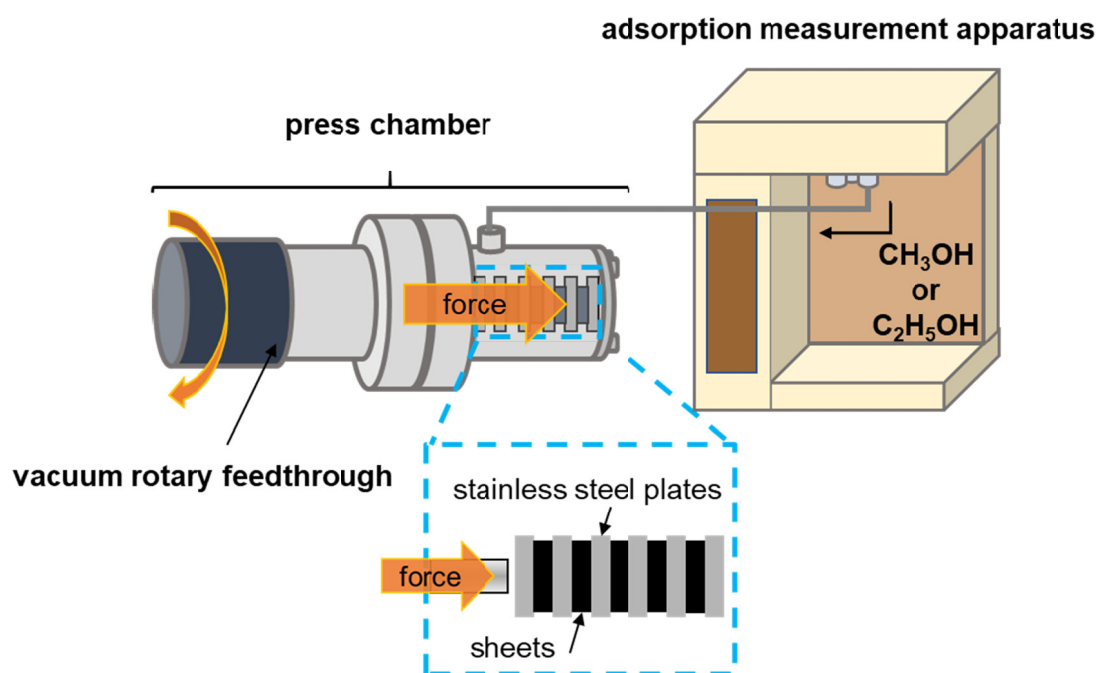
**Figure S17** (a) TG-DSC and (b) MS results of **10**.



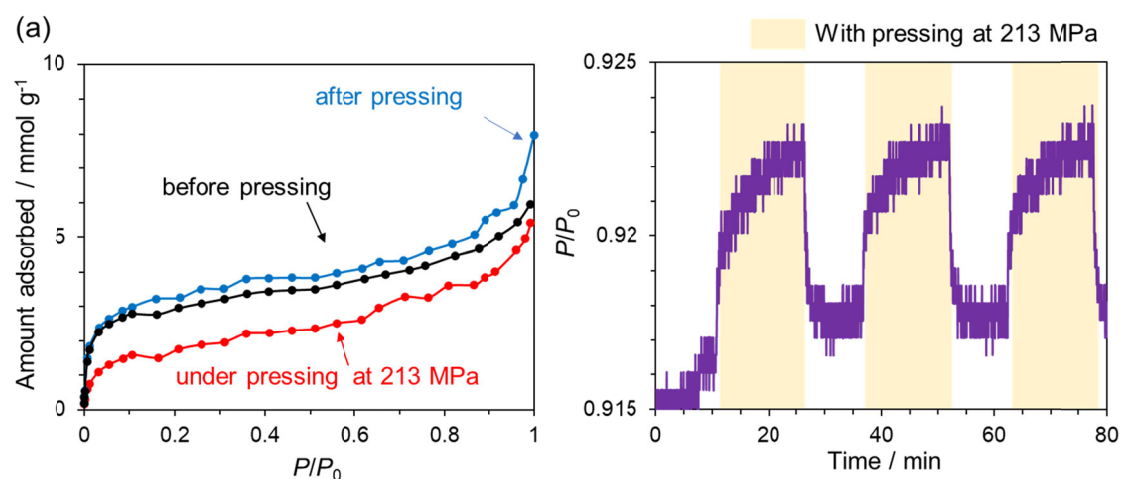
**Figure S18** PXRD patterns before and after heat treatment of **7**, **10**, and Ni-P<sub>8e</sub>.



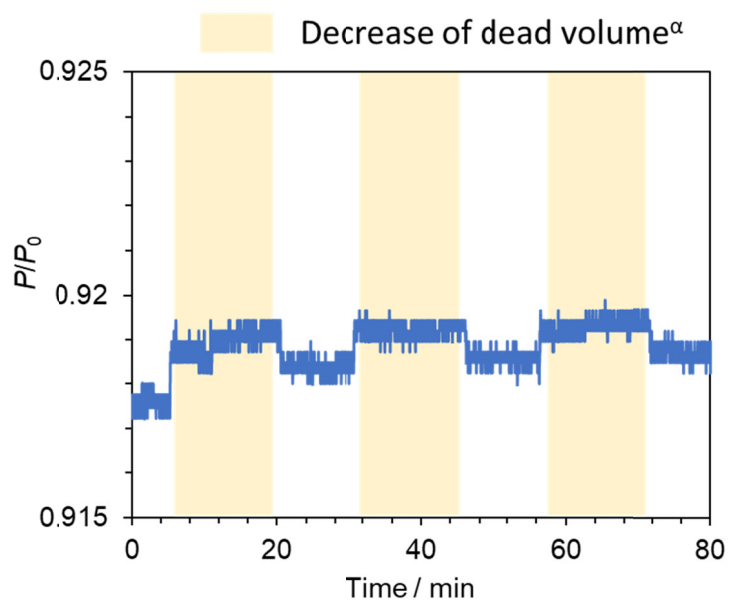
**Figure S19** (A) Structures of (a) **7**, (b) **10**, (c) Ni-P\_8e, (d) Ni-porphyrin monomer with two ethynyl groups,<sup>17</sup> and (e) Fe-porphyrin monomer with two ethynyl groups.<sup>18</sup> (B) A plot of  $S_{\text{BET}}$  of carbonized samples synthesized at 873 K versus the number of ethynyl groups in the corresponding precursors.



**Figure S20** Experimental setup for force-responsive adsorption/desorption measurement.



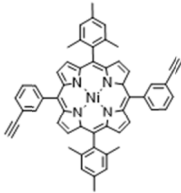
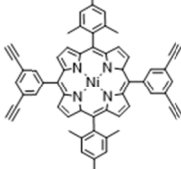
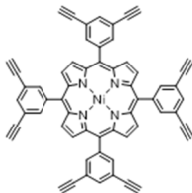
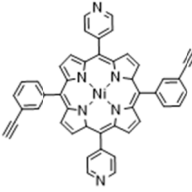
**Figure S21** (a) Ethanol adsorption isotherms (298 K) of Ni-P\_8e\_873(0) before (black), under (red) and after (blue) the application of a mechanical force (213 MPa). (b) Fluctuation of the ethanol vapour pressure ( $P/P_0$ ) inside the press chamber during applying/releasing a mechanical force (213 MPa) to Ni-P\_8e\_873(0).



**Figure S22** Fluctuation of the methanol vapour pressure ( $P/P_0$ ) inside the press chamber without Ni-P\_8e\_873(0).

<sup>α</sup> The position of the rotary feedthrough was adjusted at the same position as that during pressing.

**Table S1** Comparison of enthalpy change of thermal polymerization per 1 mol of ethynyl groups.

Sample	Enthalpy change of thermal polymerization / kJ mol <sup>-1</sup>
	11
	38
	100
	29

**Table S2** Elemental analysis results.

Sample	N / wt%	Ni / wt%
Ni-P_8e <sup>α</sup>	6.5	6.8
Ni-P_8e_873(0) <sup>β</sup>	6.0	5.3

<sup>α</sup>Theoretical values

<sup>β</sup>Determined by EDS elemental analysis



**Table S3** Structural parameters obtained from EXAFS fitting results of Ni-P\_8e and the heat-treated samples.

Sample	Shell	Coordination Number	R / Å	e <sup>0</sup> / eV	σ <sup>α</sup> / Å	R-factor / %
Ni-P_8e	Ni-N	4 <sup>β</sup>	1.96	4.9	0.050	0.79
Ni-P_8e_873(0)	Ni-N	3.9	1.89	1.6	0.069	0.78
Ni-P_8e_873(1)	Ni-N	3.5	1.86	-0.93	0.063	0.48
Ni-P_8e_973(0)	Ni-N	3.4	1.86	-3.0	0.066	0.10
	Ni-Ni	0.94	2.50	3.1	0.067	1.90

<sup>α</sup> Debye-Waller factor

<sup>β</sup> Fixed

**Table S4** Porous textures of Ni-P\_8e and carbonized samples with previous work.

Sample	$S_{\text{BET}} / \text{m}^2 \text{g}^{-1}$	$V_{\text{total}}^{\alpha} / \text{cm}^3 \text{g}^{-1}$
Ni-P_8e	11	0.02
Ni-P_8e_553(0)	55	0.03
Ni-P_8e_873(0)	605	0.29
Ni-P_8e_873(1)	673	0.35
Ni-P_8e_973(0)	267	0.12
Previous work <sup>β</sup>	276	0.18

<sup>α</sup> The total pore volume was calculated at  $P/P_0 = 0.96$ .

<sup>β</sup> OCF synthesized by carbonization of Ni porphyrin monomer (Figure S19d) at 873 K and 1 h.<sup>17</sup>

**Table S5** Porous textures of carbonized samples synthesized from different porphyrin monomers.

Sample	$S_{\text{BET}} / \text{m}^2 \text{g}^{-1}$	$V_{\text{total}}^{\alpha} / \text{cm}^3 \text{g}^{-1}$
<b>7</b> _873(0)	0	0
<b>10</b> _873(0)	41	0.04
Ni-P_8e_873(0)	605	0.29
Previous work <sup>β</sup>	276	0.18
Previous work <sup>γ</sup>	5	0

<sup>α</sup> The total pore volume was calculated at  $P/P_0 = 0.96$ .

<sup>β</sup> OCF synthesized by carbonization of Ni porphyrin monomer (Figure S19d) at 873 K and 1 h.<sup>17</sup>

<sup>γ</sup> OCF synthesized by carbonization of Fe porphyrin monomer (Figure S19e) at 873 K without keeping time.<sup>18</sup>

## References

- 1 J. D. Megiatto, R. Spencer and D. I. Schuster, *J. Mater. Chem.*, 2011, **21**, 1544-1550.
- 2 D. D. Yao, X. Zhang, O. Mongin, F. Paul and C. O. Paul-Roth, *Chem. Eur. J.*, 2016, **22**, 5583-5597.
- 3 K. Sonogashira, Y. Tohda and N. Hagihara, *Tetrahedron Lett.*, 1975, **16**, 4467-4470.
- 4 M. Ravikanth, J. P. Strachan, F. R. Li and J. S. Lindsey, *Tetrahedron*, 1998, **54**, 7721-7734.
- 5 Q. Chen, L. Brambilla, L. Daukiya, K. S. Mali, S. De Feyter, M. Tommasini, K. Mullen and A. Narita, *Angew. Chem. Int. Ed.*, 2018, **57**, 11233-11237.
- 6 C. H. Lee and J. S. Lindsey, *Tetrahedron*, 1994, **50**, 11427-11440.
- 7 V. Favre-Nicolin and R. Cerny, *J. Appl. Crystallogr.*, 2002, **35**, 734-743.
- 8 H. M. Rietveld, *J. Appl. Crystallogr.*, 1969, **2**, 65-71.
- 9 S.T. Jackson and R. G. Nuzzo, *Appl. Surf. Sci.*, 1995, **90**, 195-203.
- 10 J. Gao, Y. Wang, H. H. Wu, X. Liu, L. L. Wang, Q. L. Yu, A. W. Li, H. Wang, C. Q. Song, Z. R. Gao, M. Peng, M. T. Zhang, N. Ma, J. O. Wang, W. Zhou, G. X. Wang, Z. Yin and D. Ma, *Angew. Chem.-Int. Edit.*, 2019, **58**, 15089-15097.
- 11 Z. S. Li, L. Zhang, B. L. Li, Z. S. Liu, Z. H. Liu, H. Q. Wang and Q. Y. Li, *Chem. Eng. J.*, 2017, **313**, 1242-1250.
- 12 F. Jaouen, E. Proietti, M. Lefevre, R. Chenitz, J. P. Dodelet, G. Wu, H. T. Chung, C. M. Johnston and P. Zelenay, *Energy Environ. Sci.*, 2011, **4**, 114-130.
- 13 B. Ravel and M. Newville, *J. Synchrot. Radiat.*, 2005, **12**, 537-541.
- 14 Z. Y. Ryu, J. T. Zheng, M. Z. Wang and B. J. Zhang, *Carbon*, 1999, **37**, 1257-1264.
- 15 H. Nishihara, T. Simura, S. Kobayashi, K. Nomura, R. Berenguer, M. Ito, M. Uchimura, H. Iden, K. Arihara, A. Ohma, Y. Hayasaka and T. Kyotani, *Adv. Funct. Mater.*, 2016, **26**, 6418-6427.
- 16 K. Nomura, H. Nishihara, M. Yamamoto, A. Gabe, M. Ito, M. Uchimura, Y. Nishina, H. Tanaka, M. T. Miyahara and T. Kyotani, *Nat. Commun.*, 2019, **10**, 10.
- 17 H. Nishihara, K. Matsuura, M. Ohwada, M. Yamamoto, Y. Matsuo, J. Maruyama, Y. Hayasaka, S. Yamaguchi, K. Kamiya, H. Konaka, M. Inoue and F. Tani, *Chem. Lett.*, 2020, **49**, 619-623.
- 18 M. Yamamoto, K. Takahashi, M. Ohwada, W. Yuxin, K. Iwase, Y. Hayasaka, H. Konaka, H. Cove, D. D. Tommaso, K. Kamiya, J. Maruyama, F. Tani and H. Nishihara, *Catal. Today*, 2021, **364**, 164-171.